Canadian Conference - Pacific Conference on Earthquake Engineering 2023
Vancouver, British Columbia
June 25th – June 30th, 2023

Recent Developments in Self-Centering Piston-Based Braced Frames

Navid Rahgozar[1*], M. Shahria Alam[2]

[1]Postdoctoral Research fellow, Applied Laboratory for Advanced Materials & Structures (ALAMS), School of Engineering, The University of British Columbia, Kelowna, BC, Canada V1V 1V7.
[2] Professor and Tier-1 Principal's Research Chair in Resilient & Green Infrastructure, EME 4211, School of Engineering, The University of British Columbia, Kelowna, BC, Canada V1V 1V7
[*] E-mail: n.rahgozar@ubc.ca (Corresponding Author)

ABSTRACT

The present article introduces a novel hybrid system called Self-Centering Piston-Based Bracing Frames (SC-PBBFs) that incorporate Shape Memory Alloy (SMA) bars and Friction Springs (FSs). A capacity design procedure is presented, and the seismic performance of SC-PBBFs is compared to Buckling Restrained Braced Frames (BRBFs) in terms of collapse prevention and damage reduction. Despite the projected construction cost of SC-PBBFs being expected to exceed that of conventional bracing methods, it is imperative to investigate whether the increased upfront cost can be offset over the building's lifespan. To this end, the economic losses of low-rise building archetypes resulting from far-field earthquakes, including collapse, irreparable damage, and repair events, are quantified, considering seismic hazards, structural demands, and damage consequences. The findings reveal that the total and collapse losses of BRBFs were higher than those of SC-PBBFs, however the lower repair costs of non-structural components in BRBFs mitigated the percentage of repair losses. Furthermore, the low-rise SC-PBBF design was able to recover its initial construction expenses over its expected lifespan, in contrast to the low-rise BRBF design.

Keywords: Self-centering, piston-based brace frames, shape memory alloy, friction springs.

INTRODUCTION

The seismic design standards and building codes prioritize life-safety and structural integrity during seismic events. However, conventional code-compliant systems that rely on ductility often incur substantial permanent seismic damage to critical building elements while dissipating seismic energy. This seismic-induced residual damage can significantly disrupt building functionality and impose adverse socio-economic consequences, including repair costs and downtime. In response, sustainable design concepts rooted in performance-based seismic design and resilience-based earthquake design have emerged as promising approaches [1]. These innovative concepts aim to mitigate seismic losses and enhance functional recovery. Notable examples of resilient structural systems encompass self-centering braced frames [2], piston-based braced frames with polyurethane cores [3], stacked rocking cores [4].These sophisticated systems are engineered to effectively compensate for potential seismic damage over their service life, thereby minimizing detrimental impacts on society and the economy.This paper introduces a recent developed hybrid self-centering piston-based bracing (SC-PBB) system that incorporates super-elastic shape memory alloy (SMA) bars and friction springs (FSs). Experimental results have unequivocally demonstrated the effectiveness of SC-PBBs fitted with only FSs in mitigating residual damage through their self-centering responses [5]. To enhance the system's reliability, the combination of FS or SMA components can increase redundancy of SC-PBB in case of unexpected failure. Furthermore, the initial stiffness and energy dissipation capacity of SC-PBBs with FSs are modest, warranting the development of a novel damper that integrates both SMA bars and FSs. This proposed bracing system aims to augment the stiffness, strength, and energy dissipation capacity of existing piston-based archetypes. The components provide a backup system to safeguard against potential damage to each component during severe ground motions. Figure 1(a) illustrates a configurations of the hybrid SC-PBB assemblies, which consist of a cylinder tube, SMA bars, FSs, and a piston shaft. The archetype incorporates SMA bars and high-strength Belleville washer springs as FSs, which find applications in structural systems such as seismic isolation systems, braced frames, controlled rocking core systems, and sliding connections. The proposed hybrid SC-PBB combines the advantages of both SMA and FS assemblies, resulting in good energy dissipation capacity and minimal residual deformation under design-level ground motions. As shown in Figure 1(a), a steel shaft can move within the cylinder, activating components through piston plates confined by FS assemblies and a cylinder cover. The SMA bars are connected at both ends of the cylinder and designed to exit during compression, while couplers prevent them from fully entering during tension. Parallel and series configurations with higher numbers of stacked disks offer increased load resistance and stroke deformation.

The diagram in Figure 1(b) depicts the general responses of un-stressed and pre-stressed SMA bars and FSs in the SC-PBBs. The SMA bars are a type of smart alloy with unique characteristics, such as shape recovery after unloading. Nickel-titanium SMAs are commonly used in structural components due to their high axial tensile capacity, recoverable flexibility, and exceptional fatigue and corrosion resistance. The response of SMA bars, as shown in Figure 1(b), involves the transformation between austenite and martensite crystal phases through changes in internal forces or temperature, a phenomenon previously studied by Alam et al. [6]. The notable feature of SMA-based seismic devices, ideal for resilient structural designs, is their super-elasticity, which allows them to regain their original shape during unloading at a constant temperature. Figure 1(b) illustrates the arrangement of stacked rings with mating taper faces and the overall behavior of pre-compressed FSs. These springs are highly resistant to compressive loads. Normal and frictional forces are activated on the inclined surfaces of the rings when subjected to external forces. During compression, the subassemblies slide against each other, and the friction opposes the relative sliding motion, dissipating seismic energy. The mechanical action through the taper surfaces causes the inner rings to be squeezed while the outer rings expand concurrently. The available stroke (d_F) gradually decreases with increased compression. When all the rings collapse on each other, the FS reaches a locking position (d_{uF}-F_{uF}), resulting in a significant increase in stiffness, resembling a solid steel column. Beyond the locking point ($F > F_{uF}$), the FS follows the hysteresis of the steel material. Moreover, Figure 1(c) shows the SC-PBB responses with pre-stressed FSs and SMA bars and FSs. Pre-stressing enhances stiffness, strength, and energy dissipation of the FSs. As shown, the hysteresis of the SC-PBBF is self-center and includes elastic, hardening, and unloading branches. Post-yield strength occurs when SMAs yield or springs slide. Moreover, the building performance levels of the hybrid SC-PBBFs is shown in Figure 1(c), including operational (OP), immediate occupancy (IO), life safety (LS), and collapse prevention (CP) levels. The SC-PBBF archetype is expected to ensure self-centering response at the IO level, and provide superior performance compared to traditional structures during design-level earthquakes. The failure consequence of components depends on their ultimate capacity in the LS to CP range, where the FSs and SMAs can reach their spring lock and yield strengths, respectively, providing a safety margin against unexpected collapse.

SEISMIC DESIGN OF SC-PBBF ARCHETYPES

A design procedure is proposed for the design of SC-PBBF archetype, involving initial parameter determination, capacity design of hybrid bracings, modal analysis, stiffness verification, and allocation of strength to SMA and FS components [7]. As shown in Figure 2(a), the design considerations include story and bay dimensions, displacement requirements, geometric and design parameters for FS, cross-sectional area and number of required SMAs, brace shaft and tube design, and attachment plate strength. Step 2 of the design process involves capacity design, modal analysis, and stiffness verification for the SC-PBBF archetype. It includes determining yield strengths, estimating the fundamental period, and ensuring stiffness requirements are met. This step ensures the structure is designed to meet performance objectives and structural requirements. Step 3 involves allocating strength to SMA (F_{ds}) and FS (F_{dF}) components using the elastic axial force of the brace and proportioning their design strength (F_d) with the strength factor (η):

$$\boldsymbol{F_{\mathrm{ds}} = \eta F_{\mathrm{d}}; F_{\mathrm{dF}} = (1-\eta)F_{\mathrm{d}}; 0 < \eta < 1} \tag{1}$$

Brace deformation is approximated using story and bay dimensions, and design displacement is considered higher for large seismic demands. The design of the friction spring (FS) involves determining its contribution to lateral stiffness using geometric and design parameters. The stiffness is influenced by parameters such as taper angle, friction coefficient, number of rings, and cross-sectional area of inner and outer rings. Parallel and series arrangements can be used for increased stiffness and load resistance, and higher pre-compression force can affect stiffness and energy dissipation capacity. The required length and number of rings (n_r) of FS are determined based on available stroke (d_F), pre-compression displacement (d_{iF}) requirements, and the gap width before pre-compression (d_{r0}) [7]:

$$\boldsymbol{d_{uF} = d_{iF} + d_F = n_r d_{r0}} \tag{2}$$

The design of SMA bars involves calculating their cross-sectional area (A_s) and number (n_s) based on diameter (d_s) and pre-stressed level (η_s), martensite-to-austenite finishing stress (σ_{mf}) [7]:

$$\boldsymbol{A_s = \frac{F_{ds}}{\eta_s \sigma_{mf}}; n_s \geq \frac{4A_s}{\pi d_s^2}} \tag{3}$$

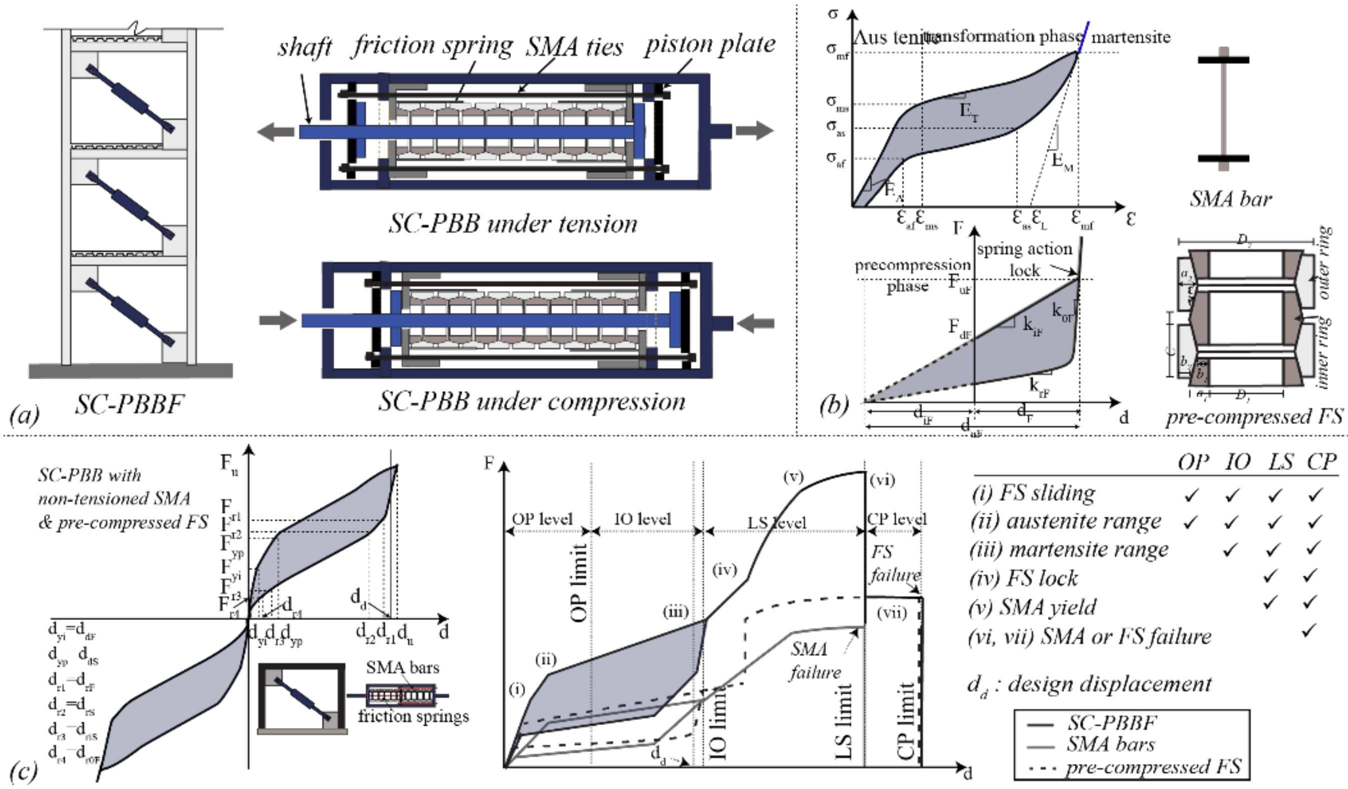

Figure 1. Details of the: (a) piston-based brace frame, (b) SMA and FS, (c) performance response.

SEISMIC PERFORMANCE EVALUATION OF ARCHETYPES

Assembling and simulation of building performance model

The proposed capacity design procedure was used to design low-rise archetypes in a high seismic risk zone of Los Angeles, California, and their design values are given in Table 1. As shown in Figure 2(b), the illustrative archetypes are in the high seismic design category (SDC) with soil site class D (SDC: D_{max}). The prototype building has rectangular floor plans with a footprint of 76 m×38 m, 7.6 m bays, and a uniform story height of 3.8 m. The seismic mass of each floor and roof is 1410 and 1255 tons, respectively. The computational modeling of archetypes using OpenSees software with nonlinear elements is depicted in Figure 2(b). A combination of SMA and FS materials was used, and a MinMax command was employed to simulate component fracture. This detailed modeling approach allows for their accurate performance assessment during seismic events. The archetypes were analyzed for 44 far-field records of 14 seismic events. The seismic hazard curves (λ_{IM}) of the studied region and recodes are shown in Figure 2(c). The hazard curves were obtained from USGS website for Beverly Hills, Los Angeles, are used for loss assessment and calculating exceedance rates for different hazard levels.

The performance model of prototype buildings equipped with SC-PBBFs and BRBFs for earthquake loss assessment involves classifying damageable components, estimating quantities of structural components from building layout, and using normative quantities for non-structural elements. Examples of fragility functions and components repair costs are shown in Figure 3. The fragility and repair cost curves are derived from the FEMA P-58 database [8], considering uncertainties and specific engineering demand parameters (EDPs) for each component. Fragility curves are related to seismic demands and associated consequences. Repair cost curves are defined using Max Cost and Min Quantity corresponding with Min Cost and Max Quantity, respectively, to account for economy of scale.

Table 1. Design information of the SC-PBBF.

Story number	F_d (kN)	F_{dS} (kN)	F_{dF} (kN)	n_s	n_r
1	963	482	482	24	38
2	866	433	433	22	28
3	667	334	334	17	18

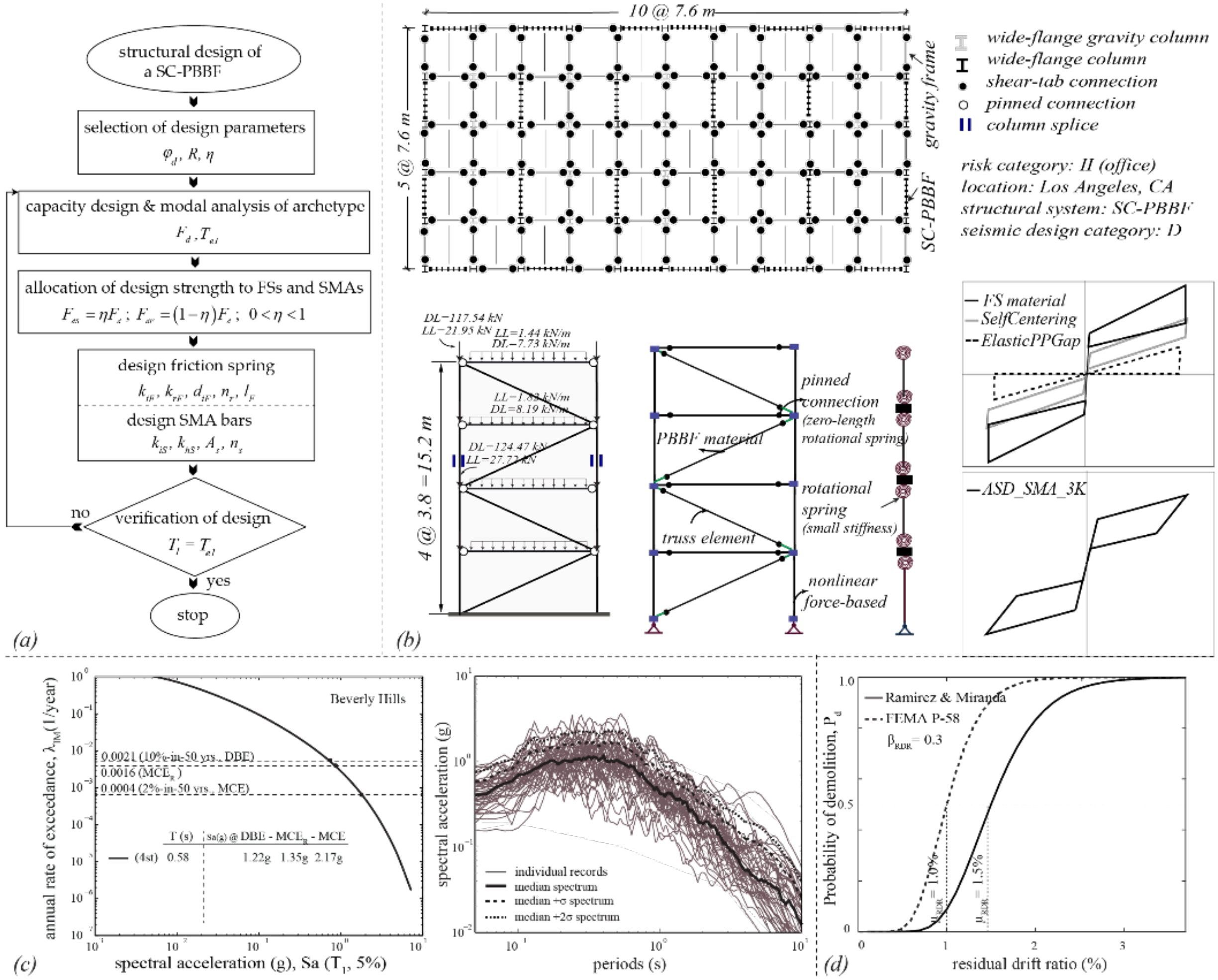

Figure 2. (a) Design procedure of SC-PBBFs, (b) configuration and simulation of the SC-PBBF archetype, (c) Site-specific seismic hazard curves, (d) Demolition fragility function.

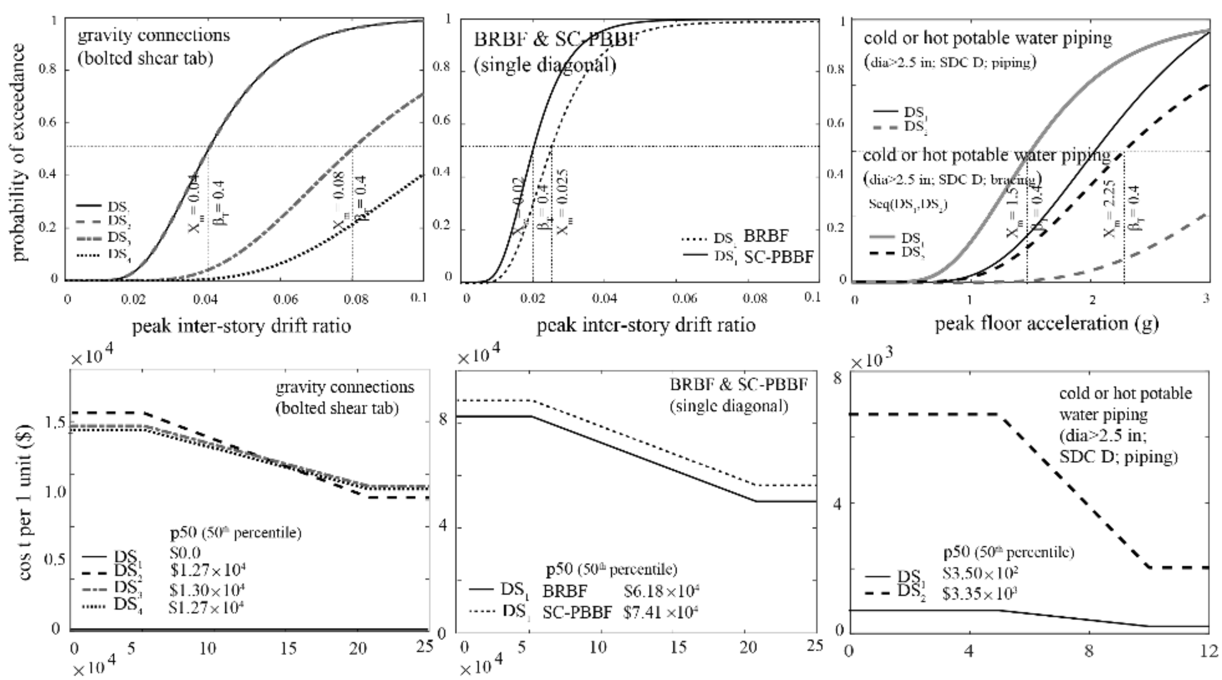

Figure 3. Component fragility curves and *component costs of prototype building.*

Collapse risk evaluation of archetypes

The FEMA P695 [9] guideline is used to assess the seismic collapse assessment of the archetypes. The collapse risk assessment involved quantifying the collapse fragility curves through incremental dynamic analysis (IDA) under 44 far-field ground motions. The collapse fragility curve was adjusted for record-to-record uncertainty and amplified using spectral shape factor (SSF) to estimate the collapse capacity. System-level uncertainties were also considered, including design requirement accuracy, test data robustness, and computational model precision. The total collapse uncertainty (β_{TOT}) was calculated using values corresponding to different quality ranks. The collapse probability of archetypes was compared against acceptance criteria of $ACMR_{10\%}$ and $ACMR_{20\%}$, which represent the median safety factor against collapse under MCE-level spectral intensity. The ACMR of individual archetypes and their average value ($ACMR_m$) must meet the acceptable criteria of $ACMR_{20\%}$ and $ACMR_{10\%}$, respectively, as specified in FEMAP695 for different collapse probabilities.

$$\mathbf{ACMR} \geq \mathbf{ACMR_{20\%}}; \mathbf{ACMR}_{\boldsymbol{m}} \geq \mathbf{ACMR_{10\%}} \tag{4}$$

Figure 4(a) illustrates the IDA curves of archetypes for peak floor acceleration (PFA), peak inter-story drift ratio (IDR), and peak residual drift ratio (PIDR) demands, and their collapse fragility curves were shown in Figure 4(b). Median collapse-level spectral intensities (S_{CT}) were determined, which the SC-PBBF provide the larger value. Collapse margin ratio (CMR) was quantified to provide safety margins against risk-targeted MCE-level intensity at fundamental period. The record-to-record uncertainty (β_{RTR}) values, calculated from IDAs by assuming a lognormal distribution, with values of 0.21 and 0.39. The design procedure was assumed to be standard, resulting in a "superior" rating for design uncertainty (β_{DR} = 0.1) requirements. High-quality test data and precise simulation in OpenSees software led to a "good" rating (β_{TD} = β_{MDL} = 0.2) for system-level uncertainty. The β_{TOT} uncertainty of SC-PBBF and BRBF was 0.37 and 0.49. Adjusted fragility curves were derived using β_{TOT} values and SSF values obtained from FEMA P695. The ACMR values for SC-PBBF and BRBF quantified as from 2.50 and 5.15, respectively. The archetypes passed the acceptance criteria, with a probability of collapse less than 20% at MCE intensity.

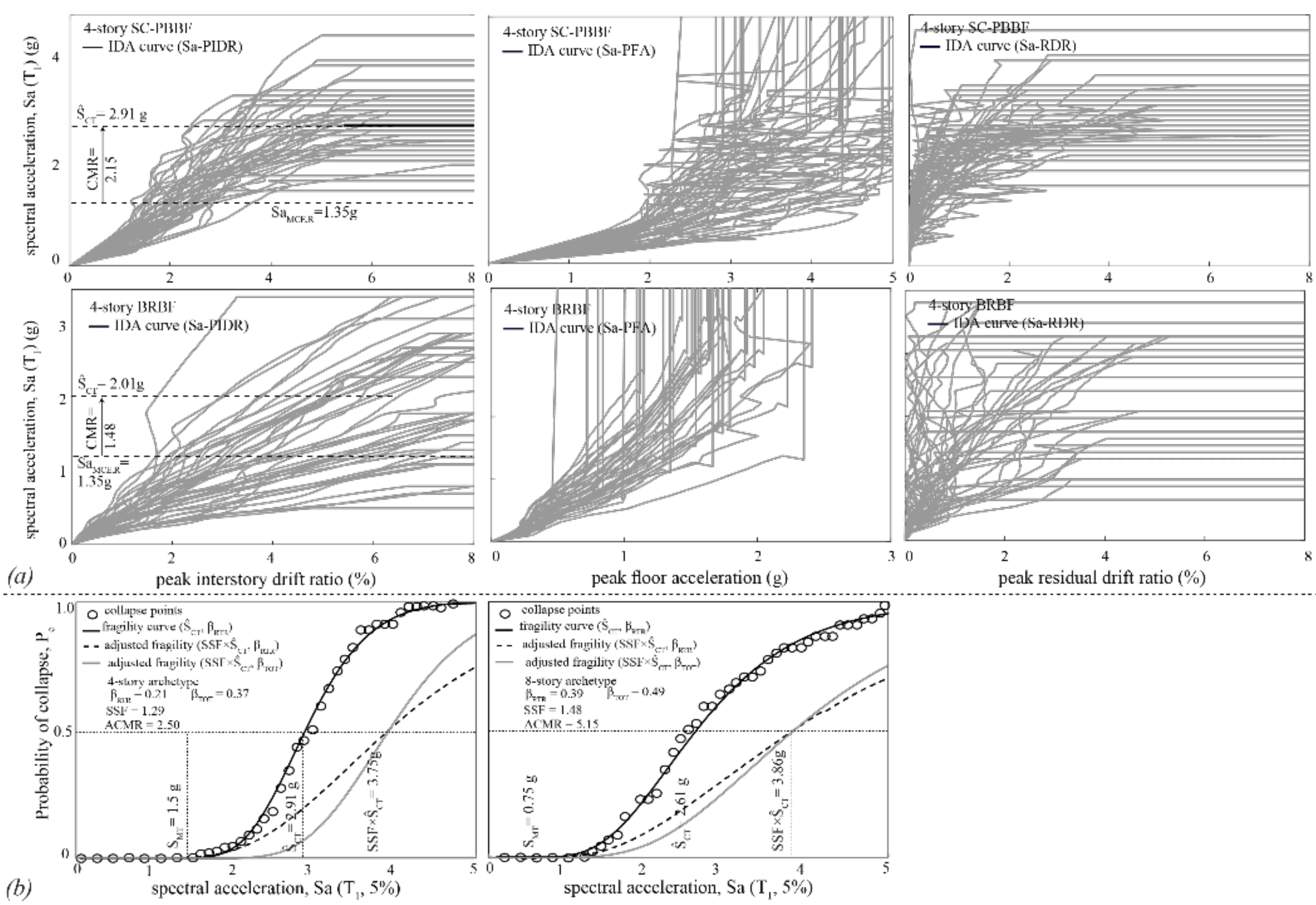

Figure 4. (a) IDA and (b) collapse fragility curves of SC-PBBF and BRBF archetypes.

Seismic loss evaluation of archetypes

The loss evaluation involved quantifying collapse, irreparable, and repair losses of the archetypes using vulnerability curves developed using structural demands and fragility curves. The procedure started with checking for collapse, followed by assessing repairability, and quantifying repair losses for both structural and non-structural elements. Seismic loss assessment should consider component-based damage at each story, as it directly affects human and financial losses. A Performance-Based Earthquake Engineering (PBEE) framework has been employed for targeting economic loss, repair time, fatalities, injuries, and other factors. This requires a loss metric such as Expected Annual Loss (EAL), which provides insights for decision-making on risk management and mitigation strategies. The process of building performance modeling for seismic loss assessment involves classifying vulnerable components, determining collapse fragility function, and quantifying expected economic loss using total probability theorem. Expected annual loss (EAL) and EAL overtime (E[L]) can be computed as decision variables by integrating over possible intensity measures, considering discount rate, time, and replacement cost. The performance model for earthquake loss assessment involves classifying damageable components, including structural and non-structural elements, into fragility curves and determining the consequences of each damage state. Quantity estimation of structural components is approximated from building layout, while normative quantities are provided for non-structural elements. Fragility functions and repair cost curves are derived from the FEMA P-58 database, considering the uncertainties and specific engineering demand parameters (EDPs) for each component.

The magnitude of seismic intensity and extent of damage to structural and non-structural components impact earthquake-induced damage. Costs associated with demolition and replacement were provided in Table 2 and Figure 5(a) compared normalized losses of SC-PBBFs and BRBFs, including total, collapse, irreparable, and repair losses, regardless of spectral acceleration. Costs for demolition of SC-PBBFs and BRBFs was \$1.7M and their replacement costs were \$33.1M and \$32.11M, respectively. As shown in Figure 5(a), the total and collapse losses of BRBFs were higher than SC-PBBFs at all seismic intensities. The collapse probability of SC-PBBFs was lower, with negligible collapse losses at lower Sa intensities. Irreparable losses for SC-PBBFs peaked at higher Sa intensities compared to BRBFs. Repair losses for SC-PBBFs were higher, with peak values at higher Sa levels compared to BRBFs. Figure 5(b) provides a detailed breakdown of the total loss for different events at Design Basis Earthquake (DBE; 10%-in-50; Return Period, RP=475 yrs.), Risk-Targeted Maximum Considered Earthquake (MCE_R; RP=623 yrs.), and the Maximum Considered Earthquake (MCE; 2%-in-50; RP=2475 yrs.) intensity levels. The repair losses are further divided into losses for Structural Components (SC), IDR-NSCs, and ACC-NSCs. The repair losses for IDR-NSCs are higher compared to SC and ACC-NSCs. However, the structural vulnerability losses are higher in BRBFs than in SC-PBBFs. Irreparable and collapse losses are negligible for SC-PBBFs at DBE and MCE_R levels due to low RDRs. The irreparable losses of the SC-PBBF are 1.6% and 33.5% of BRBF at DBE and MCER levels, respectively. Collapse losses of BRBF are 19.5 and 3.3 times those of SC-PBBF at DBE and MCE_R levels. Repair losses of SC-PBBFs exceed BRBF counterparts due to reduced permanent damage. Figure 5(c) shows the EAL values for repair, irreparable, and collapse losses, which the SC-PBBF archetype had the lower EAL for irreparable and collapse losses in structural components compared to BRBF. However, the higher EALs in non-structural elements indicated the superior IDR and ACC performance. Additionally, Figure 5(d) illustrates the expected losses of archetypes over time, considering a discount rate (Dr) of 0.5 and 1%. The analysis with these discounts revealed the higher construction costs of SC-PBBF compared to BRBF, which can be recovered within 13 and 14 years.

Table 2. Expected losses information of BRBF and SC-PBBF.

Structural type	Normalized expected loss given IM E(LT|IM), (%)														
	Collapse			Irreparable			IDR-NSC repair			ACC-NSC repair			SC repair		
	DBE	MCE_R	MCE	DBE	MCE_R	MCE	DBE	MCE_R	MCE	DBE	MCE_R	MCE	DBE	MCE_R	MCE
SC-PBBF	<1	8.0	33.5	<1	19.1	46.1	77.6	48.1	11.6	19.6	19.1	5.5	2.3	4.9	3.2
BRBF	19.5	26.7	66.7	62.0	57.0	27.0	12.8	11.0	3.8	<1	<1	<1	5.6	4.9	2.2

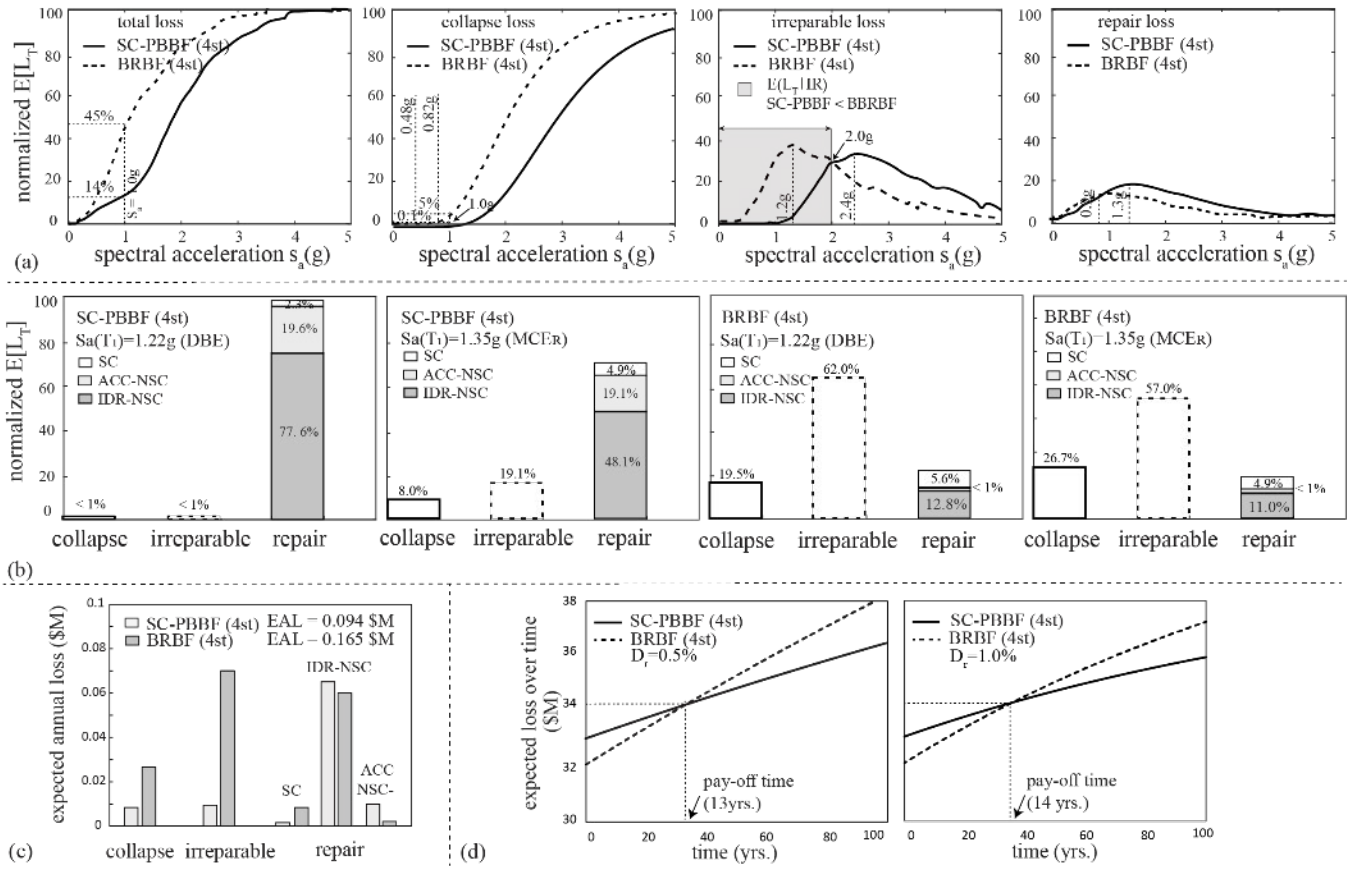

Figure 5. (a) normalized losses, (b) breakdown of the total loss, (c) the EAL values, and (d) expected losses over time.

CONCLUSIONS

This study proposed a novel earthquake-resistant system, hybrid SC-PBBFs, to enhance seismic resilience. A capacity design procedure was developed using analytical formulas, and dynamic analyses revealed the effectiveness of the proposed method. Seismic responses of low-rise SC-PBBFs are compared with conventional BRBF systems, revealing significant findings. Collapse fragility analyses were conducted for 4-story building archetypes to evaluate their collapse margin ratio against design-level intensity. Code-compliant design procedures were introduced, and OpenSees software was employed for loss evaluation. Additionally, the expected economic losses of the SC-PBBF were compared with that of BRBF counterpart using a building-specific methodology. The noteworthy findings obtained from seismic loss assessment are highlighted as follows:

• The median collapse intensity of the SC-PBBF and BRBF archetypes was 2.91 to 2.01g, respectively, and their record-to-record uncertainties and total uncertainty were ranging from 0.21-0.39 and 0.37-0.49, respectively.
• The ACMRs of the SC-PBBF and BRBF building archetypes were 2.50 and 5.15, respectively, satisfied the acceptance criteria (ACMR10% and ACMR20%).
• The SC-PBBFs experienced peak irreparable losses at spectral intensities between 2.4g, twice that of BRBFs, aligning with the lower permanent damage of SC-PBBFs. However, the SC-PBBFs incurred higher peak repair losses at larger Sa intensities compared to BRBFs.
• The disaggregation of total losses revealed that the BRBF was irreparable beyond the DBE level, experiencing large RDRs. Collapse losses for the BRBF were 19.5 and 3.3 times higher than those of SC-PBBF. In contrast, irreparable losses for the SC-PBBF were less than 1.6% and 33.5% of those of BRBFs at DBE and MCE_R levels, respectively.
• Disaggregated repair losses showed higher contributions from IDR-sensitive non-structural components compared to structural and ACC-sensitive non-structural losses.
• Construction costs of SC-PBBFs was repaid within 13-14 years for considered drifts of 0.5-1%, with increased payoff time for higher rates.

ACKNOWLEDGMENTS

Financial contributions of the Natural Sciences and Engineering Research Council (NSERC) of Canada through the Discovery Grant are gratefully acknowledged.

REFERENCES

[1] Grigorian, M., and Grigorian, C. E. (2018). “Sustainable earthquake-resisting system”. *Journal of Structural Engineering*, 144(2), 04017199.
[2] Tremblay, Robert, M. Lacerte, and C. Christopoulos. (2008). “Seismic response of multistory buildings with self-centering energy dissipative steel braces”. *Journal of structural engineering,* 134(1): 108-120.
[3] Issa, A., Rahgozar, N., and Alam, M. S. (2023). “Experimental investigation and seismic analysis of a novel self-centering piston-based bracing archetype with polyurethane cores”. *Engineering Structures*, 283, 115735.
[4] Rahgozar, N., Rahgozar, N., and Rahgozar, N. (2021). “A discontinuous cantilever beam analogy for quantifying higher mode demands in stacked rocking cores”. *The Structural Design of Tall and Special Buildings*, 30(17), e1891.
[5] Issa, Anas, Navid Rahgozar, and M. Shahria Alam. (2023). “Seismic response evaluation of spring-based piston braced frames by employing closed-loop dynamic (CLD) testing”. *Engineering Structures* 284: 115983.
[6] Alam, M. S., Youssef, M. A., and Nehdi, M. (2007). “Utilizing shape memory alloys to enhance the performance and safety of civil infrastructure: a review”. *Canadian Journal of Civil Engineering*, 34(9), 1075-1086.
[7] Rahgozar, N., and Alam, M. S., (2023). “A Novel Hybrid Self-Centering Piston-Based Bracing Fitted with SMA Bars and Friction Springs: Analytical Study and Seismic Simulation”. *Journal of Structural Engineering*, 149(6).
[8] Federal Emergency Management Agency (2018). “Seismic performance assessment of buildings”. Volume 1-Methodology. FEMA P-58-1, Washington, DC.
[9] Federal Emergency Management Agency (2009). “Quantification of building seismic performance factors”. FEMA Report P695, Federal Emergency Management Agency, Washington, DC, United States.